STATE OF THE CLIMATE IN 2021

Special Supplement to the
Bulletin of the American Meteorological Society
Vol. 103, No. 8, August 2022

Cover credits:

Flames and smoke from wildfires above the Fraser River Valley near Lytton, British Columbia, Canada, on 2 July 2021. Photographer: James MacDonald/Bloomberg ©2021 Bloomberg Finance LP - Getty

Photograph of the South Pole sunrise in September 2021. Photo taken by Jeffrey Keller, USAP/PAE, Preventative Maintenance Foreman, Colorado Springs, Colorado.

How to cite this document:

Citing the complete report:
Blunden, J. and T. Boyer, Eds., 2022: "State of the Climate in 2021". *Bull. Amer. Meteor. Soc.*, **103** (8), Si–S465, https://doi.org/10.1175/2022BAMSStateoftheClimate.1

Special Supplement to the *Bulletin of the American Meteorological Society*, Vol. 103, No. 8, August 2022 https://doi.org/10.1175/2022BAMSStateoftheClimate.1

Corresponding author: Full report: Jessica Blunden / jessica.blunden@noaa.gov

©2022 American Meteorological Society
For information regarding reuse of this content and general copyright information, consult the AMS Copyright Policy.

STATE OF THE CLIMATE IN 2021

TABLE OF CONTENTS

Abstract ..... Siii

1. Introduction S1

2. Global climate S11

3. Global oceans S143

4. The Tropics S193

5. The Arctic S257

6. Antarctica and the Southern Ocean S307

7. Regional climates S341

8. Relevant datasets and sources S455

ABSTRACT—J. BLUNDEN AND T. BOYER

In 2021, the dominant greenhouse gases released into Earth's atmosphere continued to increase. The annual global average carbon dioxide (CO_2) concentration was 414.7 ± 0.1 ppm, an increase of 2.6 ± 0.1 ppm over 2020, the fifth-highest growth rate since the start of the instrumental record in 1958. This brings the concentration of CO_2 to, once again, the highest in the modern record and ice core records dating back 800,000 years. The growth rate for methane (CH_4) was the highest on record and the third highest for nitrous oxide (N_2O), contributing to new record high atmospheric concentration levels for both gases.

Weak-to-moderate La Niña conditions were present in the eastern equatorial Pacific during most of 2021, a continuation from 2020. La Niña tends to dampen temperatures at the global scale; even so, the annual global surface temperature across land and oceans was still among the six highest with records dating as far back as the mid-1800s. While La Niña conditions contributed to Australia's coldest year since 2012, New Zealand and China each reported their warmest year on record. Europe reported its second-hottest summer on record, after 2010. A provisional new European maximum temperature record of 48.8°C was set in Sicily (Italy) on 11 August. In North America, exceptional heat waves struck the Pacific Northwest, leading to a new Canadian maximum temperature record of 49.6°C, set at Lytton, British Columbia, on 29 June, breaking the previous national record by over 4°C. In the United States, Furnace Creek in Death Valley, California, reached 54.4°C on 9 July—equaling the temperature measured at that location in 2020, which was the hottest temperature measured on Earth since 1931. The effects of warming temperatures were apparent across the Northern Hemisphere, where lakes were frozen 7.3 fewer days on average. Lake Erken, in Sweden, lost the most ice cover during the 2021 winter, with 61 days less ice cover compared to the 1991–2020 normal in response to an anomalously warm winter. The average growing season was six days longer than the 2000–20 base period. In Kyoto, Japan, full bloom dates for a native cherry tree species, *Prunus jamasakura*, were the earliest in the entire record, which began in AD 801, breaking the previous earliest date set in the year 1409.

While fewer in number and locations than record high temperatures, record cold was also observed in various locales during the year. In Spain, a new all-time national minimum temperature record of –34.1°C was set on 6 January at Clot del Tuc de la Llança in the Pyrenees. Slovenia reported a national low temperature record of –20.6°C for the month of April, set at station Nova vas Bloka.

Over Antarctica, a persistently strong and stable polar vortex helped maintain the second longest-lived ozone hole on record (shorter only than 2020), which did not close until 23 December, and contributed to the coldest extended winter on record at the South Pole. But on the northeastern Antarctic Peninsula, Esperanza and Marambio stations received persistent warm northerly winds, contributing to their warmest (tied) and second-warmest years on record, respectively.

Across the global cryosphere, glaciers lost mass for the 34th consecutive year, and permafrost temperatures continued to reach record highs at many high latitude and mountain locations. In the high northern latitudes, the Arctic as a whole (poleward of 60°N), observed its coolest year since 2013, but 2021 was still the 13th-warmest year in the 122-year record. Extreme heat events occurred during the summer. Related to the western North American heat waves, a temperature of 39.9°C was recorded in Fort Smith, Northwest Territories, Canada, on 30 June, the highest temperature ever recorded north of 60°N. A widespread melt event on the Greenland Ice Sheet on 14 August—the latest on record—coincided with the first observed rainfall in the 33-year record at the Summit Station (3216 m a.s.l.).

The seasonal Arctic minimum sea ice extent, typically reached in September, was the 12th-smallest extent in the 43-year record; however, the amount of multiyear ice—ice that survives at least one summer melt season—remaining in the Arctic at this time was the second lowest on record, indicating the Arctic's sustained transition to a younger, thinner ice cover. The oldest ice, more than four years old, has declined by 94% since the start of the record. While the rate of decline in minimum sea ice extent over the 2010–21 period has slowed compared to previous decades, Arctic sea ice volume continues to rapidly shrink.

Across the world's oceans, global mean sea level was record high for the 10th consecutive year, reaching 97.0 mm above the 1993 average when satellite measurements began, an increase of 4.9 mm over 2020. Globally-averaged ocean heat content was also record high in 2021, while the global sea surface temperature cooled compared to 2019 and 2020 due to the ongoing La Niña conditions in the tropical Pacific. Still, approximately 57% of the ocean surface experienced at least one marine heatwave in 2021.

A total of 97 named tropical storms were observed during the Northern and Southern Hemisphere storm seasons, well above the 1991–2020 average of 87, but well below the record

104 named storms of 1992. In the North Atlantic, 21 tropical cyclones formed, the third most for the basin, behind the record 30 cyclones in 2020 and 28 in 2005. There were seven Category 5 tropical cyclones across the globe—four in the western North Pacific and one each in the South Indian Ocean, Australian region, and the Southwest Pacific. Super Typhoon Rai was the third costliest typhoon in the history of the Philippines, causing about $1 billion (U.S. dollars) in damage and more than 400 deaths. While not reaching Category 5 status, Hurricane Ida was the most impactful storm in the Atlantic. At $75 billion (U.S. dollars) in damage, Ida was the costliest U.S. disaster of 2021 and the fifth most expensive hurricane on record (since 1980).

As is typical, some areas around the world were notably dry in 2021 and some were notably wet. In August, 32% of global land areas were experiencing some level of drought, a new record high. A "mega-drought" continued in central Chile for the 12th consecutive year, becoming the longest drought in the historical record in the region. Drought intensified and expanded through most of the western United States and elsewhere along a large stretch of northeastern Siberia and the Far East region of Russia, which led to unprecedented wildfires. Most of the Middle East, from Türkiye to Pakistan, also saw an intensification of drought conditions. In parts of equatorial East Africa, the annual total rainfall was the lowest on record, leading to three consecutive failed rainy seasons that resulted in one of the worst threats to food security in 35 years for more than 20 million people in the region..

Conversely, on 20 July, a 1-hour precipitation total of 201.9 mm was recorded in Zhengzhou—capital of Henan province in central China and home to more than 10 million people—the highest hourly precipitation on record for mainland China. On 4 October, a new European 12-hour rainfall record was set in Rossiglione (northwest Italy), with a total of 740.6 mm, which was more than 50% of its annual average of 1270 mm. Following months of above-average rain, the Rio Negro River at Manaus (central Brazilian Amazon) rose and remained above its emergency threshold for a total of 91 days, reaching a record high level of 30.02 m on 16 June. The overflow of the river caused damaging floods that surpassed the "once-in-a-century" Amazon flood in 2012.

STATE OF THE CLIMATE IN 2021

INTRODUCTION

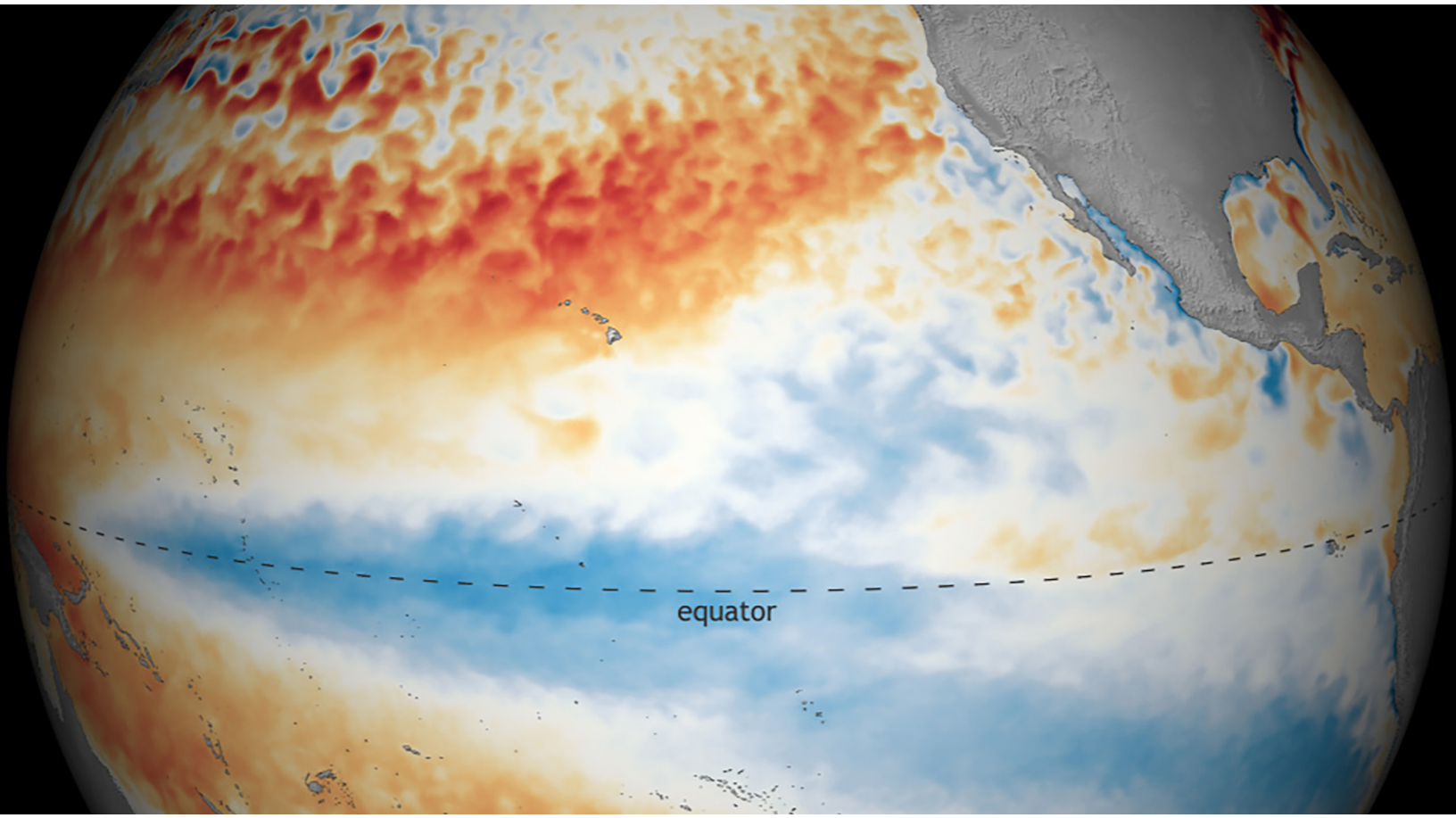

Sea surface temperature anomaly in the Pacific Ocean, December 2021 from NOAA Coral Reef Watch. Credits: NOAA Climate.gov, based on data from NOAA Coral Reef Watch

Citing this chapter: Boyer, T., J. Blunden, and R. J. H. Dunn., 2022: Introduction [in "State of the Climate in 2021"]. *Bull. Amer. Meteor. Soc.,* **103** (8), S1–S9, https://doi.org/10.1175/2022BAMSStateoftheClimate_Intro.1.

Special Supplement to the *Bulletin of the American Meteorological Society*, Vol.103, No. 8, August 2022

The Introduction is one chapter from the *State of the Climate in 2021* annual report. Compiled by NOAA's National Centers for Environmental Information, *State of the Climate in 2021* is based on contributions from scientists from around the world. It provides a detailed update on global climate indicators, notable weather events, and other data collected by environmental monitoring stations and instruments located on land, water, ice, and in space. The full report is available from https://doi.org/10.1175/2022BAMSStateoftheClimate.1.

Corresponding author, Introduction: Jessica Blunden / jessica.blunden@noaa.gov

©2022 American Meteorological Society
For information regarding reuse of this content and general copyright information, consult the AMS Copyright Policy.

STATE OF THE CLIMATE IN 2021
Introduction

Editors
Jessica Blunden
Tim Boyer

Chapter Editors

Freya Aldred
Peter Bissolli
Kyle R. Clem
Howard J. Diamond
Matthew L. Druckenmiller
Robert J. H. Dunn
Catherine Ganter
Nadine Gobron
Gregory C. Johnson
Rick Lumpkin
Ademe Mekonnen
John B. Miller
Twila A. Moon
Marilyn N. Raphael
Ahira Sánchez-Lugo
Carl J. Schreck III
Richard L. Thoman
Kate M. Willett
Zhiwei Zhu

Technical Editor
Laura Ohlmann

BAMS Special Editor for Climate
Michael A. Alexander

American Meteorological Society

Editor and Author Affiliations (alphabetical by name)

Blunden, Jessica, NOAA/NESDIS National Centers for Environmental Information, Asheville, North Carolina
Boyer, Tim, NOAA/NESDIS National Centers for Environmental Information, Silver Spring, Maryland
Dunn, Robert, J. H., Met Office Hadley Centre, Exeter, United Kingdom

Editorial and Production Team

Allen, Jessicca, Graphics Support, Cooperative Institute for Satellite Earth System Studies, North Carolina State University, Asheville, North Carolina
Hammer, Gregory, Content Team Lead, Communications and Outreach, NOAA/NESDIS National Centers for Environmental Information, Asheville, North Carolina
Love-Brotak, S. Elizabeth, Lead Graphics Production, NOAA/NESDIS National Centers for Environmental Information, Asheville, North Carolina
Misch, Deborah J., Graphics Support, Innovative Consulting and Management Services, LLC, NOAA/NESDIS National Centers for Environmental Information, Asheville, North Carolina
Ohlmann, Laura, Technical Editor, Innovative Consulting and Management Services, LLC, NOAA/NESDIS National Centers for Environmental Information, Asheville, North Carolina
Riddle, Deborah B., Graphics Support, NOAA/NESDIS National Centers for Environmental Information, Asheville, North Carolina
Veasey, Sara W., Visual Communications Team Lead, Communications and Outreach, NOAA/NESDIS National Centers for Environmental Information, Asheville, North Carolina

1. INTRODUCTION—T. Boyer, J. Blunden, and R. J. H. Dunn

The complexity of Earth's climate system was evident in 2021, as illustrated on the report's cover, with the South Pole experiencing its coldest winter on record (Sidebar 6.1), averaging –61.0°C from April through September, juxtaposed against a record high temperature for Canada of 49.6°C in the town of Lytton, northeast of Vancouver, on 29 June (Sidebar 7.1). Conditions, including a stable polar vortex and clear skies, contributed to the cold at the South Pole. A persistent high-pressure ridge over western North America, clear skies, and drought conditions contributed to 'Hell on Earth' in western Canada, to quote the title of the sidebar. However, while the year did include extremes, 2021 was overall marked more by trends ameliorated, rather than enhanced, by shorter-term phenomena, most notably the 'double dip' La Niña which persisted through the year. While ocean heat content steadily increased year over year, reaching a new high in 2021 (section 3c), indicative of steadily increasing heat in Earth's system, the annual global surface temperature was fifth or sixth highest on record (depending on the dataset referenced; section 2b) and the annual Arctic surface air temperature was the lowest since 2013 (section 5b). Chapter 3 describes the 2021 El Nino-Southern Oscillation (ENSO) state (begun in 2020) as a typical double dip La Niña, a strong La Niña interrupted (in terms of sea surface temperature threshold) by an oceanic Kelvin wave, followed by a return to La Niña conditions (Hu et al. 2014). Chapter 4 does not use the terminology but does describe the downwelling oceanic Kelvin wave which temporarily disrupted the cool near-surface waters as seen in Fig. 4.9. La Niña conditions favor enhanced Atlantic storm activity; however, in 2021, the number of named hurricanes in this basin was at the long-term mean (seven; section 4g2). Madden-Julian Oscillation (MJO) activity was low in the first part of 2021, typical for a La Niña period, with higher activity during the period of weaker/below-threshold La Niña. Other variability of note in 2021, affecting tropical and extratropical events, includes the first (weakly) negative Indian Ocean dipole since 2016 (section 4f). The complexity and evolution of Earth's climate system is cataloged here in the *State of the Climate in 2021* due to the continued dedication and efforts of the 531 authors from 66 countries representing their colleagues and contributors from universities and agencies around the globe.

"Climate is what you expect, weather is what you get" is an aphorism whose roots date back to a Mark Twain compilation of school children's sayings in the mid-1800s, but what to expect in a changing climate? The answer from the World Meteorological Organization (WMO 2007) is the climate normal—a 30-year average of a given climate variable. Since its first formalization in 1956, the climate normal has evolved into a representation of a particular mean state of a changing climate (Arguez and Vose 2011), where the differences from the previous decade's normal are assumed to be due to long-term trends. For the *State of the Climate in 2021*, many variables discussed are now compared to the most recent 1991–2020 climate normal rather than a 1981–2010 climate normal. For some variables, a 1991–2020 climate normal is not yet available or not used. For other variables, there are not yet 30 years of data for comparison; for example, mean global sea level relies on an altimeter record beginning in 1993. Given that the decadal change in the climate normal is, roughly speaking, simply a shift in the frame of reference, yearly rankings for climate variables are not affected. The status of 2021 as the sixth (or fifth) warmest year on record, as measured by global mean surface temperature, will not change regardless of whether the 1981–2010 or 1991–2020 climate normal is used as a reference. Similarly, magnitudes of year-to-year differences will not be affected, though the frame of reference has changed, in some cases significantly. For example, the annual mean surface air temperature in the Arctic is more than 0.6°C higher in the 1991–2020 climate normal than in the 1981–2010 climate normal with attendant adjustments to the reference frame of the time series of anomalies (Fig. 5.1). In 2020/21 NH lakes froze 3.8 days

later and thawed 3.5 days early vs. the 1991–2020 mean, the second shortest freeze period on record (section 2c4). In 2019/20, in comparison, NH lakes froze over 3 days later/5.5 days earlier vs. the 1981–2010 mean, third shortest on record (Sharma and Woolway 2021). A careful reading of the particular climate normal is needed to properly interpret the quantification of the climate variables in relation to interannual change. This is particularly important in variables, such as classification of ENSO conditions, which rely on a threshold value related to the mean. In fact, the trend in sea surface temperatures in the Nino-3.4 region (L'Heureux et al. 2013) necessitates a 30-year climate normal, which is modified every five years to calculate the threshold value for the Oceanic Niño Index (ONI). Without this more frequent climate normal adjustment, ENSO events defined by the ONI would not always match the physical realities of ENSO formation and consequences.

The layout of the *State of the Climate in 2021* is similar to previous years. Following this introduction (Chapter 1), Chapter 2 catalogs global climate, Chapter 3 the oceans, Chapter 4 the tropics, Chapters 5 and 6 the high latitudes (Arctic and Antarctic, respectively), and Chapter 7 other specific regions of the globe (North America, Central America/Caribbean, South America, Africa, Europe, Asia, and Oceania). Finally, Chapter 8 is a listing of many (though not all) datasets used in the various sections of the *State of the Climate in 2021* and a link to dataset access and further information. Datasets are listed by essential climate variables, with a reference to chapter(s) in which the particular dataset was used. Most of the datasets are readily downloadable by the reader who would like to reproduce the results found in this report or investigate further.

Time series of major climate indicators are again presented in this introductory chapter. Many of these indicators are essential climate variables, originally defined by the World Meteorological Organization's Global Climate Observing System (GCOS 2003) and updated again by GCOS (2010). As their name indicates, these variables are essential for a full understanding of the changing climate system. However, some of them are not available on the immediate timescales of this report, and others, particularly those dealing with the living world, are outside the scope of this report.

Essential Climate Variables—T. BOYER, J. BLUNDEN, AND R. J. H. DUNN

The following variables are considered fully monitored in this report, in that there are sufficient spatial and temporal data, with peer-reviewed documentation to characterize them on a global scale:

- Surface atmosphere: air pressure, precipitation, temperature, water vapor, wind speed and direction
- Upper atmosphere: Earth radiation budget, temperature, water vapor, wind speed and direction
- Atmospheric composition: carbon dioxide, methane and other greenhouse gases, ozone
- Ocean physics: ocean surface heat flux, sea ice, sea level, surface salinity, sea surface temperature, subsurface salinity, subsurface temperature, surface currents, surface stress
- Ocean biogeochemistry: ocean color
- Ocean biogeosystems: plankton
- Land: albedo, river discharge, snow

The following variables are considered partially monitored, in that there is systematic, rigorous measurement found in this report, but some coverage of the variable in time and space is lacking due to observing limitations or availability of data or authors:

- Atmospheric composition: aerosols properties, cloud properties, precursors of aerosol and ozone
- Upper atmosphere: lightning
- Ocean physics: subsurface currents
- Ocean biogeochemistry: inorganic carbon
- Land: above-ground biomass, anthropogenic greenhouse gas fluxes, fire, fraction of absorbed photosynthetically active radiation, glaciers, groundwater, ice sheets and ice shelves, lakes, permafrost, soil moisture
- Surface atmosphere: surface radiation budget

The following variables are not yet covered in this report, or are outside the scope of it.

- Ocean physics: sea state
- Ocean biogeochemistry: nitrous oxide, nutrients, oxygen, transient tracers
- Ocean biogeosystems: marine habitat properties
- Land: anthropogenic water use, land cover, land surface temperature, latent and sensible heat fluxes, leaf area index, soil carbon

Acknowledgments

The editors thank the BAMS editorial staff, in particular Bryan Hanssen, who provided technical guidance, oversaw publication of the report, and continues to help us shepherd the report into a digital publishing era; Liz Wright, who provided peer review support; and Nicole Rietmann, who oversaw the hundreds of citations and references this year; and the NCEI Graphics team for facilitating the construction of the report and executing the countless number of technical edits needed. We thank our technical editor Laura Ohlmann for her dedication and attention to detail. We also express our gratitude to Michael Alexander, who served as the AMS special editor for this report. Finally, we thank all of the authors and chapter editors who provide these valuable contributions each year, always with an aim to improve and expand their analyses for the readers.

Plate 1.1. Global (or representative) average time series for essential climate variables through 2021. Anomalies are shown relative to the base period in parentheses although base periods used in other sections of the report may differ. The numbers in the parentheses in the lower left or right side of each panel indicate how many in situ (red), reanalysis (blue), and satellite (orange), datasets are used to create each time series in that order. (a) NH polar stratospheric ozone (Mar); (b) SH polar stratospheric ozone (Oct); (c) surface temperature; (d) night marine air temperature; (e) lower tropospheric temperature; (f) lower stratospheric temperature; (g) extremes (warm days [solid] and cool days [dotted]); (h) Arctic sea ice extent (max [solid]) and min [dashed]); (i) Antarctic sea ice extent (max [solid] and min [dashed]); (j) glacier cumulative mean specific balance; (k) NH snow cover extent; (l) NH lake ice duration; (m) Mauna Loa apparent transmission; (n) lower stratospheric water vapor; (o) cloudiness; (p) total column water vapor – land; (q) total column water vapor – ocean; (r) upper tropospheric humidity; (s) specific humidity – land; (t) specific humidity – ocean; (u) relative humidity – land; (v) relative humidity – ocean; (w) precipitation – land; (x) precipitation – ocean; (y) ocean heat content (0–700 m); (z) sea level rise; (aa) tropospheric ozone; (ab) tropospheric wind speed at 850 hPa for 20°–40°N; (ac) land wind speed; (ad) ocean wind speed; (ae) biomass burning; (af) global land evaporation; (ag) soil moisture; (ah) terrestrial groundwater storage; (ai) fraction of absorbed photosynthetically active radiation (FAPAR); (aj) land surface albedo – visible (solid) and infrared (dashed).

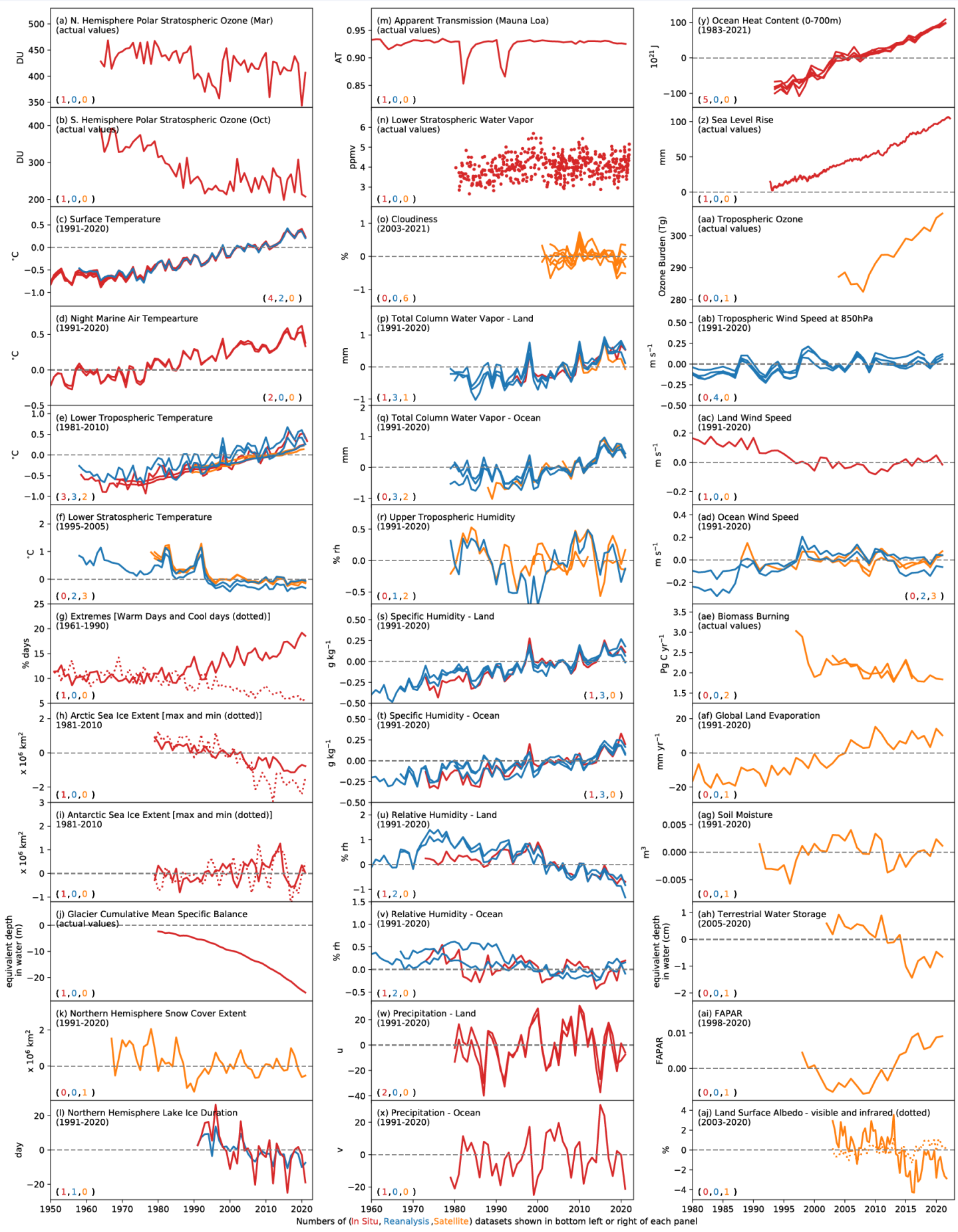
(a) N. Hemisphere Polar Stratospheric Ozone (Mar) (actual values)
DU
(1,0,0)
(b) S. Hemisphere Polar Stratospheric Ozone (Oct) (actual values)
DU
(1,0,0)
(c) Surface Temperature (1991-2020)
°C
(4,2,0)
(d) Night Marine Air Tempearture (1991-2020)
°C
(2,0,0)
(e) Lower Tropospheric Temperature (1981-2010)
°C
(3,3,2)
(f) Lower Stratospheric Temperature (1995-2005)
°C
(0,2,3)
(g) Extremes [Warm Days and Cool days (dotted)] (1961-1990)
% days
(1,0,0)
(h) Arctic Sea Ice Extent [max and min (dotted)] 1981-2010
x 10⁶ km²
(1,0,0)
(i) Antarctic Sea Ice Extent [max and min (dotted)] 1981-2010
x 10⁶ km²
(1,0,0)
(j) Glacier Cumulative Mean Specific Balance (actual values)
equivalent depth in water (m)
(1,0,0)
(k) Northern Hemisphere Snow Cover Extent (1991-2020)
x 10⁶ km²
(0,0,1)
(l) Northern Hemisphere Lake Ice Duration (1991-2020)
day
(1,1,0)
(m) Apparent Transmission (Mauna Loa) (actual values)
AT
(1,0,0)
(n) Lower Stratospheric Water Vapor (actual values)
ppmv
(1,0,0)
(o) Cloudiness (2003-2021)
%
(0,0,6)
(p) Total Column Water Vapor - Land (1991-2020)
mm
(1,3,1)
(q) Total Column Water Vapor - Ocean (1991-2020)
mm
(0,3,2)
(r) Upper Tropospheric Humidity (1991-2020)
% rh
(0,1,2)
(s) Specific Humidity - Land (1991-2020)
g kg⁻¹
(1,3,0)
(t) Specific Humidity - Ocean (1991-2020)
g kg⁻¹
(1,3,0)
(u) Relative Humidity - Land (1991-2020)
% rh
(1,2,0)
(v) Relative Humidity - Ocean (1991-2020)
% rh
(1,2,0)
(w) Precipitation - Land (1991-2020)
u
(2,0,0)
(x) Precipitation - Ocean (1991-2020)
v
(1,0,0)
(y) Ocean Heat Content (0-700m) (1983-2021)
10²¹ J
(5,0,0)
(z) Sea Level Rise (actual values)
mm
(1,0,0)
(aa) Tropospheric Ozone (actual values)
Ozone Burden (Tg)
(0,0,1)
(ab) Tropospheric Wind Speed at 850hPa (1991-2020)
m s⁻¹
(0,4,0)
(ac) Land Wind Speed (1991-2020)
m s⁻¹
(1,0,0)
(ad) Ocean Wind Speed (1991-2020)
m s⁻¹
(0,2,3)
(ae) Biomass Burning (actual values)
Pg C yr⁻¹
(0,0,2)
(af) Global Land Evaporation (1991-2020)
mm yr⁻¹
(0,0,1)
(ag) Soil Moisture (1991-2020)
m³
(0,0,1)
(ah) Terrestrial Water Storage (2005-2020)
equivalent depth in water (cm)
(0,0,1)
(ai) FAPAR (1998-2020)
FAPAR
(0,0,1)
(aj) Land Surface Albedo - visible and infrared (dotted) (2003-2020)
%
(0,0,1)
1950 1960 1970 1980 1990 2000 2010 2020
1960 1970 1980 1990 2000 2010 2020
1980 1985 1990 1995 2000 2005 2010 2015 2020
Numbers of (In Situ, Reanalysis, Satellite) datasets shown in bottom left or right of each panel

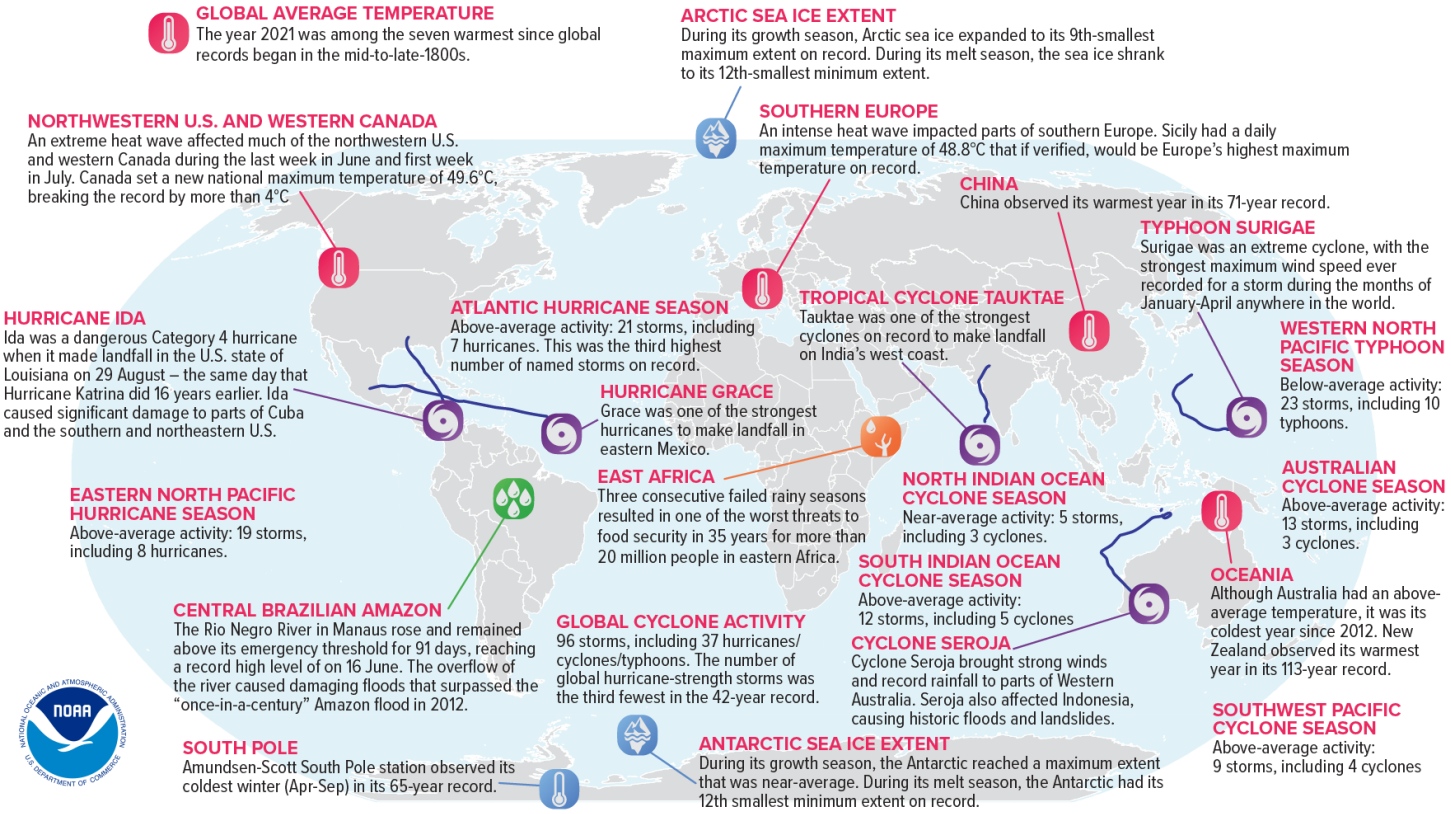

Fig. 1.1. Geographical distribution of selected notable climate anomalies and events in 2021.

References

Arguez, A., and R. S. Vose, 2011: The definition of the standard WMO climate normal: The key to deriving alternative climate normals. *Bull. Amer. Meteor. Soc*., **92**, 699–704, https://doi.org/10.1175/2010BAMS2955.1.

GCOS, 2003: The second report on the adequacy of the global observing system for climate in support of the UNFCCC. WMO/TD 1143, GCOS-82, 85 pp., https://library.wmo.int/doc_num.php?explnum_id=3931.

——, 2010: Implementation plan for the Global Observing System for Climate in Support of the UNFCCC. WMO Tech. Doc. WMO/TD-1523, 186 pp. [Available online at www.wmo.int/pages/prog/gcos/Publications/gcos-138.pdf.]

Hu, Z.-Z., A. Kumar, Y. Xue, and B. Ja, 2014: Why were some La Niñas followed by another La Niña? *Climate Dyn.*, **42**, 1029–1042, https://doi.org/10.1007/s00382-013-1917-3.

L'Heureux, M. L., D.C. Collins, and Z.-Z. Hu, 2013: Linear trends in sea surface temperature of the tropical Pacific Ocean and implications for the El Niño-Southern Oscillation. *Climate Dyn*, **40**, 1223–1236, https://doi.org/10.1007/s00382-012-1331-2.

Sharma, S., and R. I. Woolway, 2021: Lake ice, [in "State of the Climate in 2020"]. *Bull. Amer. Meteor. Soc.*, **102** (8), S48–S51, https://doi.org/10.1175/BAMS-D-21-0098.1.

WMO, 2007: The role of climatological normals in a changing climate. WMO/TD-1377, WCDMP-61, World Meteorological Organization, 130 pp., https://library.wmo.int/index.php?lvl=notice_display&id=16659.